Arabian Journal of Chemistry (2017) xxx, xxx–xxx

King Saud University

Arabian Journal of Chemistry

www.ksu.edu.sa
www.sciencedirect.com

ORIGINAL ARTICLE

Structure and composition peculiarities and spectral-luminescent properties of colorless and pink $Bi_4Ge_3O_{12}$ scintillation crystals

G.M. Kuz'micheva [a], I.A. Kaurova [a,*], L.I. Ivleva [b], E.V. Khramov [c], P.A. Eistrikh-Geller [a], V.B. Rybakov [d], T.V. Chukhlovina [b], S.V. Firstov [e]

[a] *Moscow Technological University, MITHT, 86 Vernadskogo pr., Moscow 119571, Russia*
[b] *Prokhorov General Physics Institute, Russian Academy of Sciences, 38 Vavilova Str., Moscow 119991, Russia*
[c] *National Research Center «Kurchatov Institute», 1 Akademika Kurchatova pl., Moscow 123182, Russia*
[d] *Lomonosov State University, Vorobyovy Gory, Moscow 119992, Russia*
[e] *Fiber Optics Research Center, Russian Academy of Sciences, 38 Vavilova Str., Moscow 119991, Russia*

Received 10 May 2017; accepted 25 July 2017

KEYWORDS

Scintillator;
X-ray diffraction;
EXAFS;
Point defects;
Color;
Optical properties

Abstract Czochralski-grown colorless and pink $Bi_4Ge_3O_{12}$ (BGO) single crystals have been characterized by the X-ray diffraction, X-ray absorption, and luminescence and optical spectroscopy. Additional high-temperature vacuum annealing of the as-grown colorless crystal at 900–950 °C using a special reducing agent leds to the appearance of pink coloration and modification of its properties. The refinement of actual compositions of both BGO crystals showed the distribution of the Bi^{3+} ions over two, tetrahedral and octahedral, sites, the Bi content in the colorless crystal being greater and lower in the octahedral and tetrahedral sites, respectively, compared with the colored crystal. A small amount of Bi^{5+} ions was revealed in the tetrahedral sites of the colorless crystal. Oxygen vacancies, as a part of the color center responsible for the crystal coloration, were found in the structure of pink sample. The pink BGO crystal is characterized by photoluminescence in the near infra-red spectral range.

1. Introduction

Bismuth germinate $Bi_4Ge_3O_{12}$, **BGO**, is a well known scintillation material, which is successfully used in high energy physics (calorimeters, electromagnetic spectrometers) (Grigoriev et al., 2014), medicine (positron emission tomography, computed tomography) (Hampel, 2015; Valais et al., 2010), as well as for environmental monitoring (dos Santos Júnior et al., 2017) and geological surveys (Dias et al., 2016; Weber and

* Corresponding author.
E-mail address: kaurchik@yandex.ru (I.A. Kaurova).
Peer review under responsibility of King Saud University.

Production and hosting by Elsevier

http://dx.doi.org/10.1016/j.arabjc.2017.07.015

Please cite this article in press as: Kuz'micheva, G.M. et al., Structure and composition peculiarities and spectral-luminescent properties of colorless and pink $Bi_4Ge_3O_{12}$ scintillation crystals. Arabian Journal of Chemistry (2017), http://dx.doi.org/10.1016/j.arabjc.2017.07.015

Monchamp, 1973). This material has been established to demonstrate luminescence in the near-ultraviolet and visible spectral ranges excited by ionizing radiation (vacuum ultraviolet radiation, X-rays, gamma irradiation) or charged particles (electrons, protons, ions) (Moncorge et al., 1976).

The classical and low gradient Czochralski method is usually used for growth of BGO crystals from the melt in an oxidizing atmosphere (Moncorge et al., 1976; Weber and Monchamp, 1973). Recently, the Bridgman method was applied to obtain red BGO crystals, which are characterized by the luminescence near 1500 nm. It is of interest to use these crystals as amplifiers in the optical communication systems (Yu et al., 2011a, 2014).

The $Bi_4Ge_3O_{12}$ compound crystallizes in the cubic system (sp. gr. $I\bar{4}3d$, $Z = 4$). The Ge^{4+} ions form the GeO_4 tetrahedra, and the Bi^{3+} ions form the distorted BiO_6 octahedra with different cation-anion interatomic distances CNBi = 3 + 3 (CN - coordination number) in the eulytine structure. Structural defects are associated with the Bi ions (Bravo and Lopez, 1999; Bravo et al., 1995; Kaminskii et al., 1976).

Properties of BGO crystals grown by the vertical Bridgman method in air at 1060 °C have been reported in several works (Yu et al., 2011a, 2011b, 2014). Red and white (semitransparent) crystals obtained with adding into the charge of 2 mol% and 0.5 mol% H_2O relative to GeO_2, respectively, and ordinary (clear) crystal grown from the melt without adding any components, were studied. As a result of this investigation:

- it was found that the emission intensity of red BGO at ~ 500 nm is weaker than that of ordinary BGO (Yu et al., 2011a);
- it was shown that the functions of X-ray absorption spectroscopy, both X-ray absorption near-edge structure (**XANES**) and extended X-ray absorption fine structure (**EXAFS**), are almost identical for all the samples, but a small deviation was found for the red sample, which may indicate a possible symmetry decreasing. The EXAFS Fourier transforms for the ordinary (transparent) crystal have the first peak, which characterizes the Bi-O distance of about 2.10 Å, and for the red and white crystals this distance is found to be 2.25 Å. This effect was explained by an increase in a structure disordering for the white and red BGO crystals compared with the ordinary one, which is caused by water absorption from the air by starting components before their loading into the crucible (Yu et al., 2011b);
- it was only assumed that the red color of crystals is associated with the presence of OH^{1-} groups in the growth atmosphere, which replace the O^{2-} around Bi^{3+} ions located partially in the Ge sites, forming the antisite defects according to the quasi-chemical reaction $0 \rightarrow (OH)_O^{\cdot} + Bi'_{Ge}$ (Yu et al., 2011a). An increase in the luminescence is explained by the influence of OH^- group, which is confirmed by the change in the energy level of Bi^{3+} ions (Yu et al., 2011b, 2014).

The purpose of this work is to grow colorless and colored BGO crystals by the Czochralski method and establish their actual compositions and causes of coloration.

A development of new materials with desired properties is based on the key thesis of modern crystallochemistry, namely, on finding correlations between the composition, actual structure, physical properties, and growth conditions of material. The knowledge of these correlations allows understanding the chemistry of the processes and obtaining materials with a wide range of functional properties. For the BGO crystals, a determination of actual compositions of colored and colorless crystals will allow to establish the causes of crystal coloration depending on the growth method and conditions and explain their various optical properties.

2. Experimental

2.1. Objects and methods

The colorless $Bi_4Ge_3O_{12}$ single crystal has been grown by the Czochralski method. Additional high temperature treatment (900–950 °C) of colorless sample results in obtaining the colored (pink) BGO sample. The single-crystal and powder X-ray diffraction were performed at room temperature with the Enraf-Nonius CAD-4 and HZG-4 diffractometers, respectively. The EXAFS/XANES spectroscopy of the powdered samples was carried out at room temperature at the Structural Materials Science beamline of the Kurchatov synchrotron radiation source. The transmission spectra were measured with a spectrometer PerkinElmer Lambda 900 and the luminescence and excitation spectra were recorded with an Edinburgh FLSP920 spectrofluorometer.

2.2. Synthesis procedure

The colorless optically-qualitative $Bi_4Ge_3O_{12}$ single crystal, **BGO(C)**, of 16 mm in diameter and 65 mm in length has been grown by the Czochralski method (Fig. 1a, b). It was free from cracks, bubbles, inclusions of second phases, and scattering centers and it was found to be transparent in the range of 0.35–6.5 μm, which has been detected using a Carry-5000 spectrophotometer. Under optimal conditions, the bulk crystallization rate of the crystal, grown along the [1 1 1] direction, was not exceed 0.5 cm^3/h, the axial temperature gradients in the growth and annealing zones were 80–90 °C/cm and 10–15 °C/cm, respectively.

The colored (pink) samples, **BGO(P)** (Fig. 1c), were obtained by additional high temperature treatment (900–950 °C) of plates of 1.5–2.0 mm in thickness, cut from the colorless boule, in graphite crucibles at a pressure of 10^{-2} Torr and using stannous oxalate SnC_2O_4 in an amount of several milligrams as a reducing agent. The annealing time was varied from 6 to 10 h.

2.3. Single crystal X-ray diffraction

The single-crystal X-ray diffraction (**SCXRD**) analysis of the BGO(C) and BGO(P) microcrystals of ~$0.2 \times 0.2 \times 0.2$ mm^3 in size was carried out with a Enraf-Nonius CAD-4 single-crystal diffractometer at room temperature (AgK_α, graphite monochromator, ω- scan mode). To reduce the error associated with absorption, the SCXRD data were collected over the entire Ewald sphere. The preliminary SCXRD data processing was carried out using the WinGX pack (Farrugia, 1999). The atomic coordinates, anisotropic displacements

Please cite this article in press as: Kuz'micheva, G.M. et al., Structure and composition peculiarities and spectral-luminescent properties of colorless and pink $Bi_4Ge_3O_{12}$ scintillation crystals. Arabian Journal of Chemistry (2017), http://dx.doi.org/10.1016/j.arabjc.2017.07.015

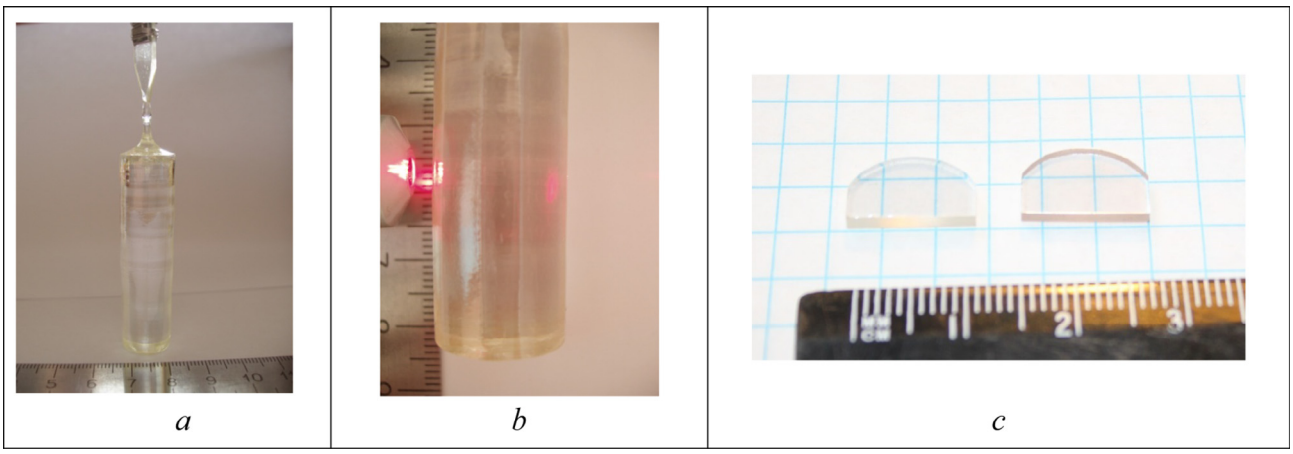

Fig. 1 Photo of colorless BGO(C) crystal (a), control of scattering centers in BGO crystal (b), and colorless BGO(C) and pink BGO(P) samples cut for investigations (c).

parameters of all atoms, and occupancies of cation and oxygen sites were refined using the SHELXL-97 software package (Sheldrick, 2008), taking into account the atomic scattering curves for neutral atoms, with the semi-empirical (azimuthal scan) (North et al., 1968) or empirical (Walker and Stuart, 1983) correction of absorption.

The structural parameters were refined in several steps. Initially, the positional and thermal parameters were simultaneously refined in the isotropic and anisotropic approximations. Then the refinement of thermal parameters together with the occupancy of octahedral site was performed with the fixed occupancies of tetrahedral (Ge) and oxygen sites. Thereafter, the occupancy of tetrahedral site was refined with the fixed occupancy of oxygen site, and vice versa. Due to the well-known correlation between thermal parameters and site occupancies we used the strategy of crystal structure refinement developed by our team for both present objects and other complex oxides and described in detail (Kaurova et al., 2010; Kuz'micheva, 2016). After each refinement step, the residual electron density, thermal parameters, and interatomic distances were analyzed. The actual compositions taking into account the electroneutrality, the correct values of the thermal parameters, the lowest values of the *R* factors, and the absence of residual electron-density peaks serve as criteria for the accuracy of the structure refinement and the correctness of the determination of the composition.

2.4. Powder X-ray diffraction

The powder X-ray diffraction analysis (**XRPD**) of ground samples (~100 mg) was carried out at room temperature on an HZG-4 X-ray powder diffractometer.

2.5. EXAFS/XANES spectroscopy

The EXAFS/XANES spectra of powdered samples (~100 mg), taken from the same part of crystals as for SCXRD experiment, were measured at room temperature at the Structural Materials Science beamline of the Kurchatov synchrotron radiation source (Trofimova et al., 2013). The samples were ground to a powder and evenly applied on the adhesive tape, having a small X-ray absorption coefficient. The sample thickness was chosen experimentally in order to provide a unit edge step, *i.e.* to make an absorption coefficient change approximately by one in natural log scale (or *e* times in linear scale) during the energy scan of near-edge range, but not to allow the absorption coefficient itself exceed 4 in log scale. The energy scans were performed using a Si(2 2 0) crystal monochromator with an energy resolution of $\Delta E/E \sim 2 \times 10^{-4}$. XAFS spectra were collected at the Bi and Ge K edges in a transmission mode, placing the sample between two ionization chambers connected to picoammeter (Keithley), which also served as a voltage source. The intensity of the monochromatic beam incident on the sample and passing through it was measured in an air ionization chamber and a chamber filled with pure Ar up to atmospheric pressure, respectively.

The standard processing of the experimental spectra was performed using the IFEFFIT program package (Ravel and Newville, 2005). The character of the atom's immediate environment was studied by analyzing the radial distribution function $\varphi(r)$, obtained by Fourier transform of the $k^3 \cdot \chi(k)$ function during the experiment, where the multiplication by k^3 was used to compensate the attenuation of the oscillations of the X-ray absorption coefficient with distance from the absorption edge.

The Fourier transforms of EXAFS oscillations were extracted in the range of the photoelectron wavenumbers (k) from 2 to 14 $Å^{-1}$ at the Ge K-edge and from 2 to 12.5 $Å^{-1}$ at the Bi L_3-edge and modelled in the range of the interatomic distances (R, Å) from 1.2 to 3.0 Å at the Bi L_3-edge, and from 1.4 to 3.6 Å at the Ge K-edge.

2.6. Optical and luminescence spectroscopy

The transmission spectra were measured in the wavelength range from 0.3 to 2 μm on a spectrometer Lambda 900 (PerkinElmer) with the scan step 1 nm. Measurements of luminescence and excitation spectra of the samples were carried out using an optical spectrofluorimeter FLSP920 (Edinburgh Instruments) with a 250 W xenon lamp operating in the wavelength range 240–850 nm. The spectral width of excitation line

Δλ was ~10 nm. The luminescence in the spectral region 240–1650 nm was detected by photomultipliers in a perpendicular configuration. The spectral resolution of the luminescence spectra obtained was 1 nm. Glass filters were used to eliminate scattered excitation radiation.

3. Results and discussion

3.1. SCXRD analysis

Fig. 2 shows the diffraction patterns of the BGO powders made of the single crystals. Their indexing confirms that the BGO samples under investigation are isostructural and belong to the eulytine structure (JCPDS №89-1419). A shift for the reflections at high 2θ angles evidences most likely the difference in the unit cell parameters. In turn, the difference in the unit cell parameters found for BGO(C) and BGO(P), both for powdered samples and microcrystals (Fig. 3), evidences the difference in their actual compositions.

Tables 1 and 2 show the experimental parameters and the results of refinement of BGO(C) and BGO(P) crystal structures, and Table 3 shows their refined actual compositions, namely, $(Bi_{3.994}\square_{0.006})(Ge_{2.980(48)}Bi_{0.020})O_{12.00}$ – for the colorless BGO(C) crystal and $(Bi_{3.987(45)}\square_{0.013})(Ge_{2.988(35)}Bi_{0.012})(O_{11.98(5)}\square_{0.02})$ – for the pink BGO(P) crystal (vacancies are denoted by squares, □).

As can be seen from the refined compositions, both crystals contain defects (Table 3). The unit cell parameters of these crystals are less than those found for the defect-free $Bi_3Ge_4O_{12}$ crystals, grown by the Czochralski and hydrothermal methods and investigated by the neutron diffraction including the refinement of site occupancies (Radaev et al., 1990). Analysis of the compositions of microcrystals (without standard deviations) allowed to reveal: a small deficiency of oxygen sites ($V_O^{\cdot\cdot}$) in the BGO(P) structure and the absence of O vacancies in the BGO(C) crystal; vacancies in the Bi sites ($V'_{Bi}{}^{m}$) in both structures (greater for the BGO(P) microcrystal); the presence of Bi in tetrahedral Ge sites, i.e. antisite defect Bi'_{Ge} (with the assumption that Bi has formal charge 3+) for both crystals

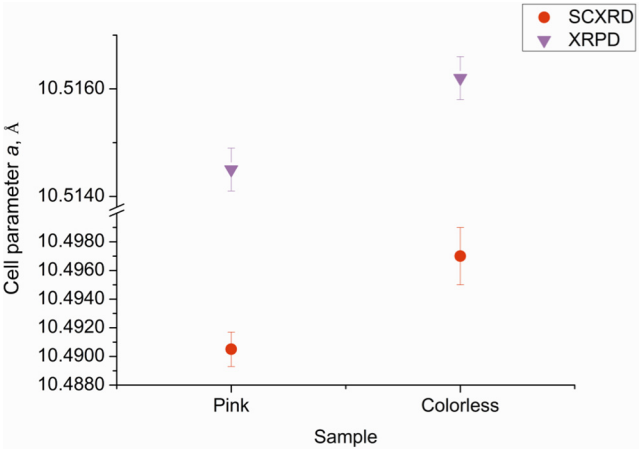

Fig. 3 The unit cell parameters for BGO(C) and BGO(P) samples according to SCXRD (microcrystals) and XRPD (powdered crystals).

(greater for the BGO(C) sample); the higher Bi content in the BGO(C) microcrystal compared with the BGO(P) one.

The distorted BiO_6 polyhedron with the different cation-anion distances (Bi-3O2 > Bi-3O1) is a characteristic feature of the $Bi_3Ge_4O_{12}$ crystal structure (Fig. 4a). The distortion is due to the lone active pair of electrons (*E*-pair), the location of which is detected by the analysis of the residual electron density ($x = y = z = 0.9389$) in the structure of BGO(C) sample (Fig. 4b).

According to the calculation of the degree of distortion (δ) of the BiO_6 polyhedron using the formula $\delta = \Sigma\Delta d_i^2/(CN - 1)$ (Δd is a difference in distances between the vertices of a distorted and ideal coordination polyhedron; the i is changed from 1 to CN), its value in the structure of BGO(P) sample ($\delta = 1.534$) is found to be lower than that in the BGO(C) structure ($\delta = 1.855$). It is due to the presence of O vacancies ($V_O^{\cdot\cdot}$) in the structure of BGO(P) sample, which reduce the action of the active *E*-pair and contribute to the symmetrization of polyhedron.

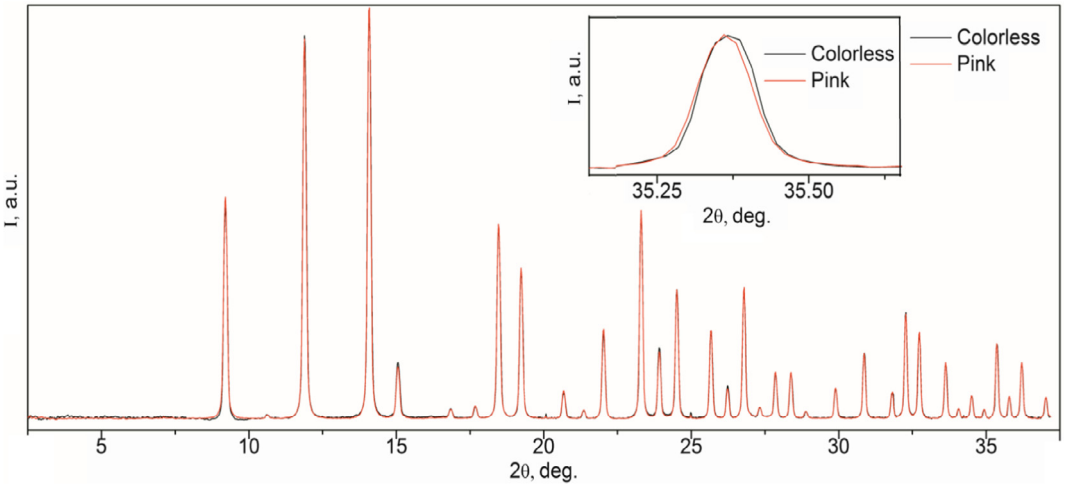

Fig. 2 Diffraction patterns of BGO powders made of the single crystals (λ = 0.6889 Å). Box gives the reflection profile for BGO(C) and BGO(P).

Please cite this article in press as: Kuz'micheva, G.M. et al., Structure and composition peculiarities and spectral-luminescent properties of colorless and pink $Bi_4Ge_3O_{12}$ scintillation crystals. Arabian Journal of Chemistry (2017), http://dx.doi.org/10.1016/j.arabjc.2017.07.015

Table 1 Crystallographic data, experimental details and parameters of BGO crystal structure refinement according to the SCXRD data.

Sample	BGO(C)	BGO(P)
Chemical formula of the nominal composition	$Bi_4Ge_3O_{12}$	
System, Space group, Z	Cubic, $I\bar{4}3d$, 4	
a, Å	10.497(2)	10.491(1)
V, Å^3	1156.63(1)	1154.49(1)
D_x, g cm^{-3}	7.155	7.168
Radiation λ, Å	Ag$K\alpha$; 0.55940	
Absorption, μ, mm^{-1}	37.29	37.36
T, K	295	
Sample size, mm	~0.2 × 0.2 × 0.2	
Diffractometer	CAD-4	
Type of scan	ω	
θ_{max}, deg	34.765	34.79
Limits h, k, l	$-19 \le h \le 19$, $-19 \le k \le 19$, $-19 \le l \le 19$	
No. of reflections: measured/unique ($I > 2\sigma(I)$)	20009/842	15412/842
No. of parameters in refinement	20	18
Weighting scheme	$1/[\sigma^2(F_0^2) + (0.0353P)^2 + 55.27P]$ $P = (F_0^2 + 2F_c^2)/3$	$1/[\sigma^2(F_0^2) + (0.0344P)^2 + 36.42P]$
R_1 ($I > 2\sigma(I)$)	0.0331	0.0298
wR_2	0.0798	0.0740
S	1.029	1.061
Program	SHELXL-97	

Table 2 Coordinates of atoms and their equivalent thermal parameters $U_{eq} \times 10^2$ (Å^2), site occupancies p (SOF) and main interatomic distances d (Å) in the structures of BGO crystals according to the SCXRD data.

Parameter	Sample	
	BGO(C)	BGO(P)
Bi1 (16c)		
x	0.91248(2)	0.08751(2)
y	0.91248(2)	0.08751(2)
z	0.91248(2)	0.08751(2)
p	0.3328(33)	0.3322(38)
U_{eq}	0.43(1)	0.39(1)
Ge, Bi2 (12a)		
x	0	0
y	3/4	1/4
z	5/8	3/8
Ge		
p	0.2483(25)	0.2490(29)
U_{eq}	0.31(9)	0.22(3)
Bi2		
p	0.0017(25)	0.0010(29)
U_{eq}	2.4(2)	2.2(2)
O(48e)		
x	0.9299(8)	0.0695(8)
y	0.8732(8)	0.1260(7)
z	0.7123(7)	0.2875(6)
p	1.00	0.998(5)
U_{eq}	1.0(1)	0.9(1)
Bi – 3 × O (O1)	2.150(7)	2.144(7)
– 3 × O (O2)	2.609(8)	2.602(7)
$[Bi\text{-}O]_{avr}$	2.380	2.373
Ge – 4 × O	1.747(7)	1.751(7)
Bi – 3 × Bi	3.5859(7)	3.5747(7)
– 3 × Bi	3.6812(7)	3.6732(7)
$[Bi\text{-}Bi]_{avr}$	3.6336	3.6240
O2–Ge–O2	105.9(2)	105.9(2)
O2–Ge–O2	116.7(5)	116.8(5)
O1–Bi–O2	84.2(1)	84.2(1)
O1–Bi–O2	70.7(3)	70.2(3)
O1–Bi–O1	85.1(1)	85.4(3)
O2–Bi–O2	114.0(1)	114.0(1)

Table 3 Characteristics and refined compositions of the BGO microcrystals.

Initial charge composition	Refined composition (SCXRD)[a]	Color
$Bi_4Ge_3O_{12}$ BGO(C)	$(Bi_{3.994(40)}\square_{0.006})[Ge_{2.980(30)}Bi_{0.020})O_{12.00}$	Colorless
$Bi_4Ge_3O_{12}$ BGO(P)	$(Bi_{3.987(45)}\square_{0.013})(Ge_{2.988(35)}Bi_{0.012})(O_{11.98(5)}\square_{0.02})$	Pink

[a] Vacancies are denoted by squares, □.

The GeO_4 tetrahedra have equal cation-anion distances (Fig. 4c) with different O-Ge-O bond angles (Table 2). The distorted BiO_6 octahedron is connected with the vertices of the GeO_4 tetrahedra by the O2 atoms, the most distant from Bi atoms (Fig. 4d), and with other BiO_6 polyhedron by an edge (Fig. 4e). The GeO_4 and BiO_6 polyhedra are connected with each other by their vertices to form the chains (Fig. 4f) due to the connection between the vertices of three GeO_4 tetrahedra, and four Bi polyhedra, and the edges of two BiO_6 polyhedra. The coordination number of oxygen atoms is three (CNO = 3): the O atoms are coordinated by two Bi atoms and one Ge atom.

The refined compositions of Bi crystallographic site correlate with the interatomic distances in the BiO_6 polyhedron (Table 2): the average Bi-O distance in the structure of BGO (C) sample with less concentration of defects in the Bi site is higher than the same distance in the structure of BGO(P) sample. However, the cation-anion distance in the GeO_4 tetrahedron is slightly lower in the structure of BGO(C) crystal compared with the same distance in the structure of pink BGO(P) one with less Bi content in the tetrahedral sites (rBi > rGe, r – radius of ion). Such a behavior of the interatomic distances can be explained by the mutual influence of polyhedra on each other (a decrease in the Bi-O2 interatomic distance in the BiO_6 polyhedron increases the Ge-O interatomic distance in the GeO_4 polyhedron), as it was

Please cite this article in press as: Kuz'micheva, G.M. et al., Structure and composition peculiarities and spectral-luminescent properties of colorless and pink $Bi_4Ge_3O_{12}$ scintillation crystals. Arabian Journal of Chemistry (2017), http://dx.doi.org/10.1016/j.arabjc.2017.07.015

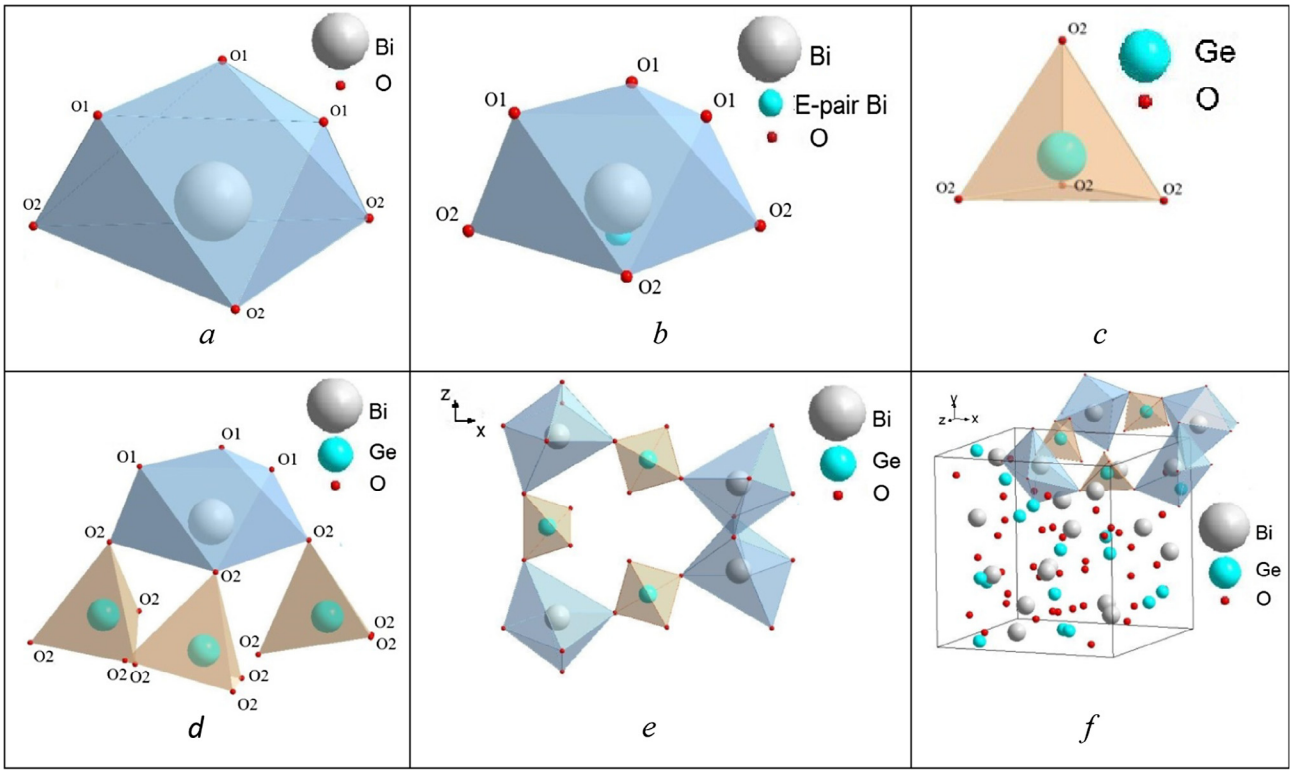

Fig. 4 The BiO_6 polyhedron (a), the BiO_6 polyhedron with an active lone pair of electrons (b), the GeO_4 polyhedron (c), the connection between BiO_6 and GeO_4 polyhedra (d, e), and the unit cell of $Bi_4Ge_3O_{12}$ (f).

observed in the structure of defect-free $Bi_3Ge_4O_{12}$ crystal with increasing temperature (Radaev et al., 1990).

There is also another explanation for such a behavior of the interatomic distances in the BGO structures. The presence of the Bi^{3+} ions in the tetrahedral sites is highly problematic due to the large cation size ($rBi^{3+} \sim 0.85$ Å). At the same time, the presence of the Bi^{5+} ions ($rBi^{5+} \sim 0.60$ Å) in the tetrahedral sites, especially together with the other ions with the smaller sizes (Craig and Stephenson, 1975), is justified in terms of the crystallochemical point of view. According to the oxygen radius ($R \sim 1.38$ Å), the atoms in the tetrahedral sites may have dimensions $r \sim 0.27 \div \sim 0.57$ Å. On the other hand, based on the well-known Magnus-Goldschmidt rule, the tetrahedral coordination is stable in the range of r/R from 0.225 to 0.414 (r - cation radius, R - anion radius) for preferably ionic crystals. It follows that the cations with the $r \sim 0.31 \div \sim 0.57$ Å may be located in the center of tetrahedron, which is consistent with the above-mentioned limit ($r \sim 0.27 \div \sim 0.57$ Å), taking into account the limitations for such calculations (Kuz'micheva, 2016).

3.2. XRPD analysis

The full-profile refinement of structures of BGO single crystals (Fig. 1c) ground to a powder is performed using a MRIA program (Zlokazov and Chernyshev, 1992). Due to the strong correlation between the structural parameters (atomic coordinates, atomic displacements, and occupancies), the site occupancies of all the atoms have not been refined. However, when the atomic displacements for O atoms and the site occupancies for all atoms are fixed to be $B_{iso}(O) = 1.00$ and $p = 1$, respectively, the refined atomic displacements for the Bi and Ge atoms have the following values: $B_{iso}(Bi) = 0.34(2)$ Å^2 and $B_{iso}(Ge) = 0.51(3)$ Å^2 - for the BGO(C) sample, and $B_{iso}(Bi) = 0.23(2)$ Å^2 and $B_{iso}(Ge) = 0.14(3)$ Å^2 - for the BGO(P) sample. In this case, it can be concluded that the greater Bi content ($N_{Bi} = 83$, N is an atomic number in the Periodic Table) is in the Ge site ($N_{Ge} = 32$) of BGO(C) structure compared with the BGO(P) one, which is consistent with the results of SCXRD analysis (Table 3).

3.3. EXAFS/XANES spectroscopy

According to the XRPD data obtained for the BGO single crystals ground to a powder, an average size of crystallites for both samples can be estimated as hundreds of nanometers, hence, the content of surface atoms is sufficiently low. Therefore, it can be assumed that the change in the amplitude of EXAFS oscillations, which determine the intensity of peaks on the curves of quasi-radial electron density distribution and the average values of coordination numbers (CN) obtained as a result of the simulation of EXAFS spectra, are not related to a dispersity and due only to the differences between crystal structures of pink and colorless BGO crystals.

The XANES spectra measured for the BGO(C) and BGO (P) samples at both edges are almost identical (Fig. 5). The small shift of ~0.5 eV in the absorption edge towards lower energies, found for the BGO(P) sample, could mean a decrease in the average formal charge (FC) of Bi (the method does not allow to distinguish similar atoms in different sites) (Fig. 5).

Please cite this article in press as: Kuz'micheva, G.M. et al., Structure and composition peculiarities and spectral-luminescent properties of colorless and pink $Bi_4Ge_3O_{12}$ scintillation crystals. Arabian Journal of Chemistry (2017), http://dx.doi.org/10.1016/j.arabjc.2017.07.015

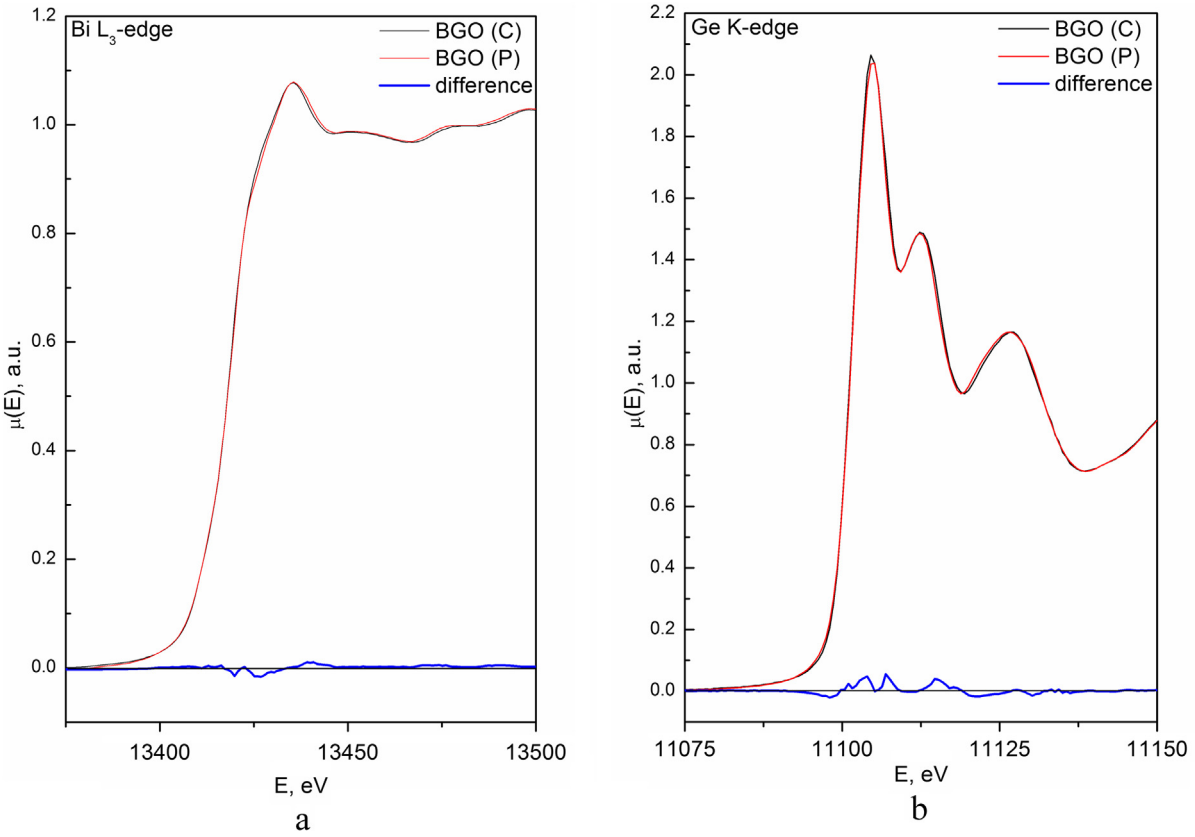

Fig. 5 The XANES spectra, measured at the Bi L_3-edge (a) and Ge K-edge (b) for BGO(C) and BGO(P) crystals.

However, this shift is below the energy resolution of monochromator: $\Delta E/E \sim 2 \times 10^{-4}$ gives $\Delta E \approx 2.6$ eV at $E \approx 13$ keV; repeated measurements do not lead to reproducible shift values but indicate that for the BGO(P) sample the absorption jump lies in the lower energy region. If only it is not caused by inaccuracy of measurements or sample preparation procedures, such a decrease can be explained by a different distribution of Bi atoms over two crystallographic sites with different FCs, Bi^{5+} and Bi^{3+}. The Bi^{5+} content is found to be lower in the pink BGO(P) crystal compared with the colorless BGO(C) one. Based on the XANES curves at the Bi L_3-edge (Fig. 5a), the greater content of the Bi^{3+} ions in the BiO_6 sites and lower content of the Bi^{5+} ions in the GeO_4 sites was found for the BGO(P) sample compared with the BGO(C) one. Moreover, due to the fact that there are only Bi^{3+} ions in the distorted octahedron (due to its crystallochemical properties), the Bi ions with FC > 3 occupy tetrahedral site together with the Ge ions, which is consistent with the interatomic distances in the tetrahedron (Table 2).

A similar result was obtained for the phase $Bi_{24}Mn_2O_{40}$ with the sillenite structure (sp. gr. *I*23; the Bi^{3+} ions with the active lone pair of electrons are located in semi-octahedral sites and the Mn^{5+} ions are in the tetrahedra) (Mel'nikova et al., 2011): the presence of Bi cations in an amount up to 10% was revealed in the tetrahedral sites using the XANES/EXAFS spectroscopy. The EXAFS spectrum of this sample at the Bi L_3-edge is well reproduced in the event that one additional interatomic distance Bi-O ~ 1.90 Å is added to a description model together with three initial Bi-O distances (2.07–2.56 Å). In the XANES spectra at the Bi L_3-edge, a slight shift towards higher energies was revealed for the $Bi_{24}Mn_2O_{40-\delta}$ sample with respect to the spectrum of defect-free $Bi_{24}^{3+}Si_{2.00(4)}^{4+}O_{40}$ sample, which is due to the appearance of Bi atoms in the tetrahedral sites, i.e. $Bi_{24}(Bi,Mn)_2O_{40-\delta}$. It should be noted that the average FC of Bi in the $Bi_{24}(Bi,Mn)_2O_{40-\delta}$ is higher than that in the $Bi_{24}^{3+}Si_{2.00(4)}^{4+}O_{40}$. This fact indicates that the FC of Bi in the tetrahedral site of $Bi_{24}(Bi,Mn)_2O_{40-\delta}$ structure is higher than 3+, i.e. $Bi^{3+\delta}$. The XANES/EXAFS results together with the results of X-ray analysis of sillenite-family single crystals show that the concentration of these ions in the tetrahedral sites should not exceed ~0.25 FU (FU is a formula units) (Mel'nikova et al., 2014). It should be noted that the possibility of the presence of Bi^{3+} ions together with the Bi^{5+} ions in the tetrahedral sites of sillenite structure has been described in several works, in particular (Craig and Stephenson, 1975; Harwig, 1978).

Based on the above-mentioned XANES data, the peak on the curve of quasi-radial electron density distribution at the Bi edge, corresponding to the Bi-O distance, is to be more intense in the structure of pink BGO(P) crystal than that in the colorless BGO(C) one. In the curve at the Ge K-edge (Fig. 5b), on the other hand, the changes in oxygen peak are to be minor, as all Ge atoms are located in the tetrahedra in the structures of both samples. Similarly, an increase in the Bi content in the special tetrahedral Ge sites should lead to an increase in the intensity peaks for the Bi-Bi (at the Bi L_3-edge) and Ge-Bi (at the Ge K-edge) distances. In turn, the intensity of Bi-Ge and Ge-Ge peaks should be decreased

Please cite this article in press as: Kuz'micheva, G.M. et al., Structure and composition peculiarities and spectral-luminescent properties of colorless and pink $Bi_4Ge_3O_{12}$ scintillation crystals. Arabian Journal of Chemistry (2017), http://dx.doi.org/10.1016/j.arabjc.2017.07.015

due to the fact that the portion of heavy Bi atoms in the Ge sites is reduced. All the above-mentioned changes are correlated with the EXAFS data (Fig. 6).

There are challenges in the quantitative interpretation of EXAFS at the Bi L_3-edge, caused by the Bi location in two different crystallographic sites and asymmetry of the local environment of Bi in the Ge sites (Fig. 6a). Coordination environment of Bi in the GeO_4 includes three close O atoms (Bi-O_{close} ~ 2.15 Å) and three more distant O atoms (Bi-O_{far} ~ 2.60 Å). Close and distant O atoms are to be described by two independent scattering paths. Hence, a model with three independent scattering paths is to be used for a correct description of the most intense Bi-O peak. The location of Bi atoms in the Ge sites should not be taken into account due to the fact that the typical values of accuracy make up more than 10% (when determining the CN of atom according to the EXAFS data). In this case, only two scattering paths, corresponding to the octahedral oxygen environment of Bi atoms, should be included into the model. The parameters of this model are shown in Table 4. The CNs for close and distant O atoms were equated to simplify the model according to reasons related to large size of the particles (see above). Giant values of the Debye parameter for distant O atoms are not caused by any errors in measurement or simulation: the forced reduction of these values (for example, by equating to the Debye parameters made for close O atoms) leads to an increase in the *R*-factor (reliability factor) up to a few percent, and an independent determination of CN leads to incorrect values, which are significantly greater than the bulk values for a perfect crystal. Such high values of the Debye parameter can be easily explained by the fact that the distant O atoms, which form the Bi environment, are, at the same time, close neighbors of the Ge atoms. In case of the partial substitution of Ge atoms by the Bi ones (antisite point defects, Bi'_{Ge}), these O atoms should be shifted significantly. It follows that an increase in the Debye parameter is not associated with the thermal fluctuations of atoms, but it is probably due to the point defects in the crystal structure. A small value of the Debye parameter, defined for the same atoms from the EXAFS spectrum at the Ge edge, confirms this assumption (Table 5).

A decrease in the content of Bi^{5+} ions in the BGO(P) crystal compared with the BGO(C) one (Table 3) can be explained by the growth of BGO(P) crystal in a reducing atmosphere:

$$\begin{aligned} Sn^{2+}C_2O_4 \rightarrow\ & Sn^{2+}O + (Bi_{3.994\square 0.006}) \\ & \times [Ge_{2.980(48)}(Bi^{3+}_{1-y}Bi^{5+}_{y})_{0.020}]O_{12.00}(BGO(C)) \\ \rightarrow\ & Sn^{4+}O_2 + (Bi_{3.987(45)\square 0.013}) \\ & \times [Ge_{2.988(35)}(Bi^{3+}_{1-z}Bi^{5+}_{z})_{0.012}](O_{11.98(5)\square 0.02}) \\ & \times (BGO(P)) \text{ with } y > z. \end{aligned}$$

It should be noted that the refinement of the BGO(P) crystal structure, taking into account that the Sn ions can partially occupy tetrahedral or octahedral sites, resulted in incorrect thermal parameters.

Thus, an investigation of the statistical crystal structure of colorless BGO(C) and colored (pink) BGO(P) crystals by the full-profile method (powdered crystals) and X-ray diffraction analysis (microcrystals), as well as an investigation of the local structure of crystals by the X-ray absorption spectroscopy, allows to obtain a general picture of the defect formation in the samples under investigation: $0 \rightarrow V'^{\,m}_{Bi} + Bi'_{Ge} + Bi^{p}_{Bi}$ - for BGO(C) crystal and $0 \rightarrow V'^{\,m}_{Bi} + Bi'_{Ge} + Bi^{p}_{Bi} + V^{n}_{O} + ne'$ or $0 \rightarrow V'^{\,m}_{Bi} + Bi'_{Ge} + Bi^{p}_{Bi} + (V^{n}_{O}, ne')^{\times}$ - for BGO(P) crystal

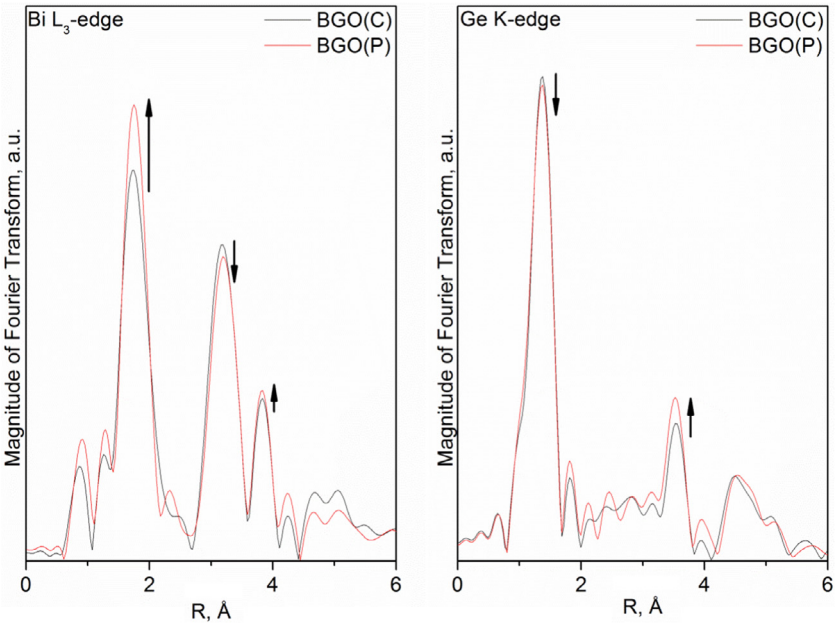

Fig. 6 EXAFS Fourier transforms, measured at the Bi L_3-edge (a) and Ge K-edge (b) for BGO(C) and BGO(P) crystals. The first peak corresponds to the oxygen environment of both atoms (single scattering path for photoelectrons M-O, M = Bi, Ge), the second and the third peaks (for Bi) correspond to M-Bi and M-Ge. The arrows show the behavior of the spectra intensity.

Please cite this article in press as: Kuz'micheva, G.M. et al., Structure and composition peculiarities and spectral-luminescent properties of colorless and pink $Bi_4Ge_3O_{12}$ scintillation crystals. Arabian Journal of Chemistry (2017), http://dx.doi.org/10.1016/j.arabjc.2017.07.015

Table 4 Results of EXAFS data modeling for the Bi L_3-edge in the range of distances R = 1.2–2.6 Å: R, interatomic distance (the length for single scattering path); CN, coordination number; σ^2, the Debye–Waller factor; O_{close} and O_{far}, close and distant oxygen atoms (see Fig. 4).

Sample	Scattering path	R, Å	CN	σ^2, Å^2	R_f, %
BGO(C)	Bi–O_{close}	2.16	2.9	0.0039	1.4
	Bi-O_{far}	2.60	2.9	0.0103	
BGO(P)	Bi-O_{close}	2.17	2.5	0.0015	1.0
	Bi-O_{far}	2.62	2.5	0.0105	

Table 5 Results of EXAFS data modeling for the Ge K-edge in the range of distances R = 1.0–2.2 Å: R, interatomic distance (the length for single scattering path); CN, coordination number; σ^2, the Debye–Waller factor.

Sample	Scattering path	R, Å	CN	σ^2, Å^2	R_f, %
BGO(C)	Ge - O	1.76	4.0	0.0022	1.27
BGO(P)	Ge - O	1.76	4.1	0.0024	1.82

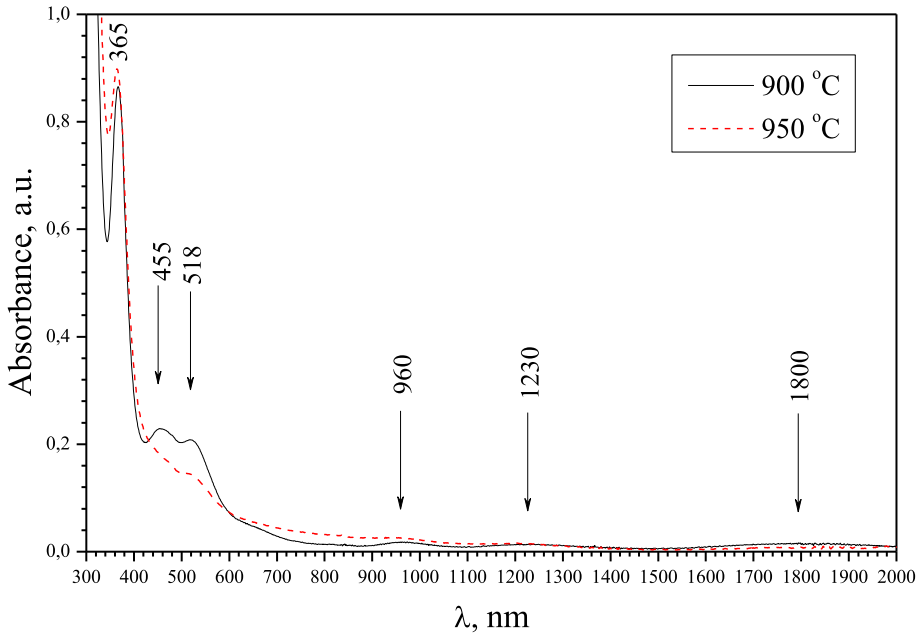

Fig. 7 Absorption spectra of the colored BGO(P) crystal after the vacuum annealing of the colorless BGO(C) crystal in the graphite crucible at 900 and 950 °C.

taking into account the color center $(V_O^{\cdot n}, ne')^{\times}$. The similar change in color from colorless to pink, found for the $Gd_3Ga_5O_{12}$ crystals with the garnet structure, was also caused by the presence of the color center $(V_{\ddot{O}}, 2e')^{\times}$ (F-center) (Kuz'micheva et al., 1988).

3.4. Optical and luminescent properties

The colorless BGO crystals are transparent in the spectral range of 0.35–6.5 μm. The BGO(P) crystal, having specific pink color, is characterized by a series of absorption bands in the visible range at 365, 455, and 518 nm and by weak absorption bands at 960, 1230, and 1800 nm (Fig. 7).

A luminescence in the visible region at 480–500 nm and its absence in the infrared region have been revealed for the colorless BGO crystals (Atroschenko et al., 1998). For the pink-colored BGO(P) sample, treated in vacuum in a graphite crucible, two luminescence peaks, the broad one at 1000–1100 nm and the narrow one at 1500 nm, were detected (Fig. 8). The excitation spectrum of the luminescence band at 1030 nm consists of the narrow band peaked at 370 nm, whereas one of the luminescence band at 1500 nm has the broad band at 450 nm. It should be noted that the presented excitation spectra consist of the overlapping bands. As a consequence, both the luminescence bands appeared at 400-nm excitation (Fig. 8). Also, when excitation wavelength was

Please cite this article in press as: Kuz'micheva, G.M. et al., Structure and composition peculiarities and spectral-luminescent properties of colorless and pink $Bi_4Ge_3O_{12}$ scintillation crystals. Arabian Journal of Chemistry (2017), http://dx.doi.org/10.1016/j.arabjc.2017.07.015

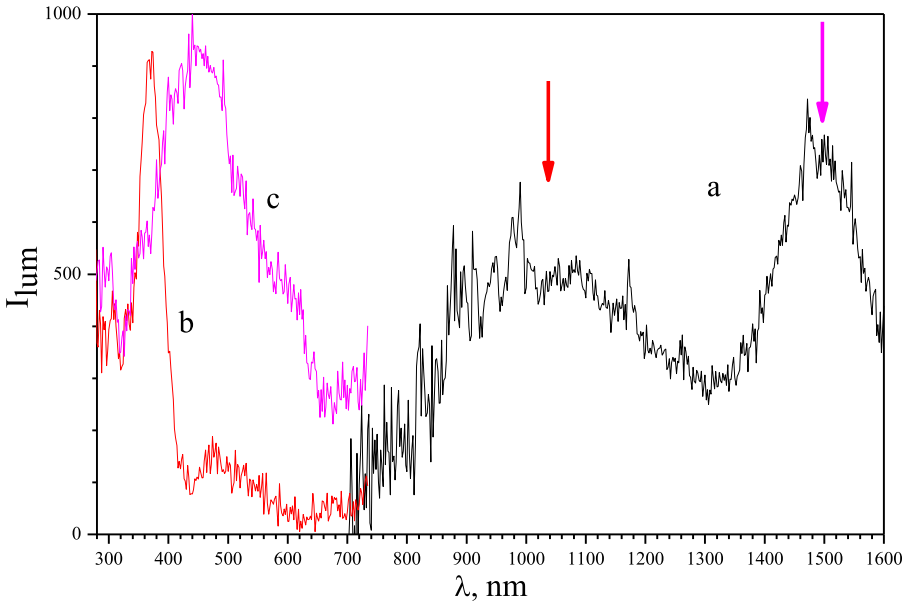

Fig. 8 Luminescence spectrum excited at 400 nm (a) and excitation spectra of 1030 (b) and 1500-nm (c) luminescence of the colored BGO(P) crystal obtained by vacuum annealing of the colorless BGO(C) crystal in the graphite crucible at 900 °C.

varied, both the luminescence bands were also observed whereas their luminescence intensity ratio changed. The occurrence of infrared luminescence at 1000–1100 and 1500 nm was observed only for the colored (pink) BGO(P) samples.

4. Conclusions

The colorless and colored $Bi_4Ge_3O_{12}$, BGO, crystals have been grown by the Czochralski method, the pink color of crystals was achieved by an additional annealing in a reducing atmosphere in graphite crucibles. The temperature-time interval for synthesis of colored BGO crystals using a special reducing agent, stannous oxalate, was determined. The actual compositions of the crystals, taking into account the composition of each crystallographic site, have been determined by the single-crystal X-ray diffraction analysis and confirmed by the powder X-ray diffraction and X-ray absorption spectroscopy. In the structures of both crystals, the Bi ions are distributed over two, octahedral and tetrahedral, sites. The greater and lower Bi content were found in the octahedral and tetrahedral sites of colorless crystal structure, respectively, compared with the pink crystal, in which the Bi^{5+} content is reduced due to the reducing treatment atmosphere. Oxygen vacancies were detected in the structure of the pink crystal, which coloration is due to the presence of color centers, the associates of an oxygen vacancy and an electron localized near it. The results of investigation of $Bi_4Ge_3O_{12}$ single crystals are in a good agreement with the results of investigation of sillenite-type single crystals and other complex oxides, having similar structural features with the eulytine structure.

Acknowledgements

The reported study was supported by the RAS Presidium Program III.2.7 and Russian Foundation for Basic Research [Research Project No. 16-33-00497].

References

Atroschenko, L.V., Burachas, S.F., Gal'chinetskii, L.P., Grinev, B.V., Ryzhikov, B.D., Starginskii, N.G., 1998. Crystals of Scintillators and Detectors of Ionizing Radiations on their Base. Naukova Dumka, Kiev.

Bravo, D., Lopez, F.J., 1999. The EPR technique as a tool for the understanding of laser systems, the case of Cr^{3+} and Cr^{4+} ions in $Bi_4Ge_3O_{12}$. Opt. Mater. 13, 141–145.

Bravo, D., Martin, A., Kaminskii, A.A., Lopez, F.J., 1995. EPR spectra of Cr^{3+} ions in $LiNbO_3$:ZnO and $LiNbO_3$:CaO. Radiat. Eff. Defects Solids 135, 261–264.

Craig, D.C., Stephenson, N.C., 1975. Structural studies of some body-centered cubic phases of mixed oxides involving Bi_2O_3: the structures of $Bi_{25}FeO_{40}$ and $Bi_{38}ZnO_{60}$. J. Solid State Chem. 15, 1–8.

Dias, F., Lima, M., Sanjurjo-Sanchez, J., Alves, C., 2016. Analysis of spectra from portable handheld gamma-ray spectrometry for terrain comparative assessment. J. Environ. Radioact. 154, 93–100.

dos Santos Júnior, J.A., dos Santos Amaral, R., Menezes, R.S.C., et al, 2017. Influence of terrestrial radionuclides on environmental gamma exposure in a uranium deposit in Paraiba Brazil. Ecotoxicol. Environ. Saf. 141, 154–159.

Farrugia, L.J., 1999. *WinGX* suite for small-molecule single-crystal crystallography. J. Appl. Cryst. 32, 837–838.

Grigoriev, D.N., Danevich, F.A., Shlegel, V.N., Vasiliev, Y.V., 2014. Development of crystal scintillators for calorimetry in high energy and astroparticle physics. J. Instrum. 9, C09004.

Hampel, U., 2015. X-ray computed Tomography. In: Wang, M. (Ed.), Industrial Tomography: Systems and Applications. Elsevier, pp. 175–196.

Harwig, H.A., 1978. On the structure of bismuthsesquioxide: the α, β, γ, and δ-phase. Z. Anorg. Allg. Chem. 444 (1), 151–166.

Kaminskii, A.A., Schultze, D., Hermoneit, B., et al, 1976. Spectroscopic properties and stimulated emission in the 4F3/2 → 4I11/2 and 4F3/2 → 4I13/2 transitions of Nd3+ions from cubic Bi4Ge3O12 crystals. Phys. Status Solidi A 33, 737–753.

Kaurova, I.A., Kuz'micheva, G.M., Rybakov, V.B., Dubovsky, A.B., Cousson, A., 2010. Composition, structural parameters, and color of langatate. Inorg. Mater. 46 (9), 988–993.

Kuz'micheva, G.M., Kozlikin, S.N., Zharikov, E.V., et al, 1988. Point defects in gadolinium-gallium garnet. Zh. Neorg. Khim. 33 (9), 33–39 (in Russsian).

Kuz'micheva, G.M., 2016. Some Aspects of the Applied Crystallochemistry. MIREA, Moscow (in Russian).

Mel'nikova, T.I., Kuz'micheva, G.M., Rybakov, V.B., Bolotina, N.B., Dubovsky, A.B., 2011. Synthesis, composition, and structure of sillenite-type solid solutions in the Bi_2O_3–SiO_2–MnO_2 system. Inorg. Chem. 50 (5), 2002–2009.

Mel'nikova, T.I., Kuz'micheva, G.M., Bolotina, N.B., et al, 2014. Structural features of compounds of the sillenite family. Crystallogr. Rep. 59 (3), 353–361.

Moncorge, R., Jacquier, B., Boulon, G., 1976. Temperature dependent luminescence of bismuth germanate ($Bi_4Ge_3O_{12}$) discussion on possible models. J. Lumin. 14, 337–348.

North, A.C.T., Phillips, D.C., Mathews, F.S., 1968. A semi-empirical method of absorption correction. Acta Cryst. A24, 351–359.

Radaev, S.F., Muradyan, L.A., Kargin, Yu.F., et al, 1990. Neutron diffraction study of $Bi_4Ge_3O_{12}$ single crystals with the eulytine structure. Kristallografiya 35 (2), 361–364 (in Russsian).

Ravel, B., Newville, M., 2005. ATHENA, ARTEMIS, HEPHAESTUS: data analysis for X-ray absorption spectroscopy using IFEFFIT. J. Synchrotron Radiat. 12, 537–541.

Sheldrick, G.M., 2008. A short history of SHELX. Acta Cryst. A64, 112–122.

Trofimova, N.N., Veligzhanin, A.A., Murzin, V.Yu., Chernyshov, A. A., Khramov, E.V., Zabluda, V.N., Edel'man, I.S., Slovokhotov, L., Yu Zubavichus, Y.V., 2013. Structural diagnostics of functional nanomaterials with the use of X-ray synchrotron radiation. Nanotechnologies Russ. 8, 396–401.

Valais, I., Michail, C., David, S., Liaparinos, P., Fountos, G., Paschalis, T., Kandarakis, I., Panayiotakis, G., 2010. Comparative Investigation of Ce^{3+} doped scintillators in a wide range of photon energies covering X-ray CT, nuclear medicine and megavoltage radiation therapy portal imaging applications. Trans. Nucl. Sci. 57 (1), 3–7.

Walker, N., Stuart, D., 1983. An empirical method for correcting diffractometer data for absorption effects. Acta. Crystallogr. A39, 158–166.

Weber, M.J., Monchamp, R.R., 1973. Luminescence of Bi_4 Ge_3 $_{O1}2$: spectral and decay properties. J. Appl. Phys. 44, 5495–5499.

Yu, P., Su, L., Wang, Q., et al, 2011a. Near-infrared luminescence of red $Bi_4Ge_3O_{12}$ down to a temperature of 8 K. Nucl. Instrum. Methods Phys. Res. 631, 40–42.

Yu, P., Su, L., Zhao, H., et al, 2011b. Spectroscopic properties of red $Bi_4Ge_3O_{12}$ by vertical Bridgman method. Opt. Mater. 33, 831–835.

Yu, P., Su, L., Zhao, H., Xu, J., 2014. Optical and structural characterization of colored $Bi_4Ge_3O_{12}$ crystals. J. Lumin. 154, 520–524.

Zlokazov, V.B., Chernyshev, V.V., 1992. MRIA-a program for a full profile analysis of powder multiphase neutron-diffraction time-of-flight (direct and Fourier) spectra. J. Appl. Crystallogr. 25, 447–451.

Please cite this article in press as: Kuz'micheva, G.M. et al., Structure and composition peculiarities and spectral-luminescent properties of colorless and pink $Bi_4Ge_3O_{12}$ scintillation crystals. Arabian Journal of Chemistry (2017), http://dx.doi.org/10.1016/j.arabjc.2017.07.015